Dynamics of Dipole-Inverted *cis*-Polyisoprene Chains in a Matrix of Long, Entangling Chains. 2. Effects of Constraint Release on the Coherence of the Subchain Motion

Hiroshi Watanabe,* Yumi Matsumiya, and Kunihiro Osaki

Institute for Chemical Research, Kyoto University, Uji, Kyoto 611, Japan

Ming-Long Yao

Rheometric Scientific F.E. Ltd, 2-19-6 Yanagibashi, Taito-ku, Tokyo 111, Japan

Received January 16, 1998; Revised Manuscript Received August 11, 1998

ABSTRACT: For *cis*-polyisoprene (PI) chains having dipoles parallel along their backbone, viscoelastic relaxation reflects orientational anisotropy of subchains (stress-generating units) at respective times while the dielectric relaxation reflects orientational correlation of the subchains at two separate times. This difference between viscoelastic and dielectric relaxation processes enables us to examine the short-time coherence of subchain motion in individual chains through comparison of these processes. Specifically, for the two extreme cases of perfectly coherent or incoherent subchain motion, viscoelastic moduli G^*_{coh} and G^*_{incoh} are explicitly calculated from the relaxation times τ_p and eigenfunctions f_p defined for a local correlation function describing fundamental features of the dielectric relaxation. On the basis of these backgrounds, the G^*_{coh} and G^*_{incoh} were calculated for a PI chain ($M = 48800$) *dilutely* blended in a high-M entangling polybutadiene (PB) matrix ($M = 263000$). (The τ_p and f_p data necessary for this calculation were obtained dielectrically in Part 1 of this series of papers.) The G^*_{coh} was in excellent agreement with the G^* data of the PI chain while G^*_{incoh} was significantly different from the data, meaning that the subchain motion was highly coherent for the PI chain in the high-M PB matrix. In contrast, the subchain motion of the same PI chain was found to be incoherent in an entangling PB matrix of smaller M (=9240). The constraint release mechanism made a negligible contribution to the global dynamics of the PI chains in the high-M matrix while it dominated the dynamics in the low-M matrix. These results indicate that the constraint release is an important factor that determines the degree of coherence of the subchain motion.

I. Introduction

For *cis*-polyisoprene (PI) chains having dipoles parallel along their backbone, slow dielectric relaxation due to the global chain motion has been extensively studied in a variety of environments.[1−18] To describe this relaxation, we divide the PI chain into N segments. On time scales longer than a characteristic time t_e for equilibration within the segment, the dielectric features of the PI chain are described in terms of the equilibrium motion of these segments. Thus, the segment size can be arbitrarily chosen according to the time scale of out interest, and the Gaussian segments (or subchains) having no isochronal orientational correlation are often used for description of the dielectric features of the PI chains.[17] Since each segment has the dipole parallel or antiparallel to its bond vector (end-to-end vector), all fundamental features of the slow dielectric relaxation of the PI chains (on time scales $> t_e$) are described by a local correlation function:[6]

$$C(n,t;m) = (1/a^2)\langle \mathbf{u}(n,t)\cdot\mathbf{u}(m,0)\rangle \qquad (1)$$

Here, $\mathbf{u}(n,t)$ is a bond vector for the nth segment at a time t and $a^2 = \langle \mathbf{u}^2\rangle$.

The local correlation function $C(n,t;m)$ can be decomposed into eigenmodes having the eigenfunctions $f_p(n)$ and relaxation times τ_p:[6]

$$C(n,t;m) = \frac{2}{N}\sum_{p=1}^{N} f_p(n)\, f_p(m)\, \exp[-t/\tau_p] \qquad (2)$$

The $f_p(n)$ and τ_p can be determined from dielectric data of a series of specially designed PI chains having the same M but differently once-inverted dipoles.[6] We synthesized this series of dipole-inverted PI chains (with $M \cong 50000$) and determined $f_p(n)$ and τ_p for the slowest three eigenmodes ($p = 1-3$) of the chains in the monodisperse bulk state,[6] in solutions,[10] and in a matrix of short, entangling polybutadiene (PB) chains (B9; $M = 9240$).[15]

In Part 1 of this series of papers,[18] we have determined $f_p(n)$ (in an integrated form) and τ_p of the dipole-inverted PI chains in a *high-M* entangling PB matrix (B263; $M = 263000$). The PI/B263 blends are chemically identical to the previously examined PI/B9 blends,[15] but the dynamics of the dilute PI probes is quite different in these blends. The *constraint release* (CR) mechanism (probe relaxation induced by matrix diffusion)[20−22] makes a negligible contribution to the PI relaxation in the B263 matrix while it dominates the relaxation in the B9 matrix.[18] Despite this difference in the CR contribution, $f_p(n)$ ($p = 1-3$) are almost identical and the decay of the τ_p/τ_1 ratio with p is nearly the same in the two matrices.[18] We also established the nonsinusoidal feature of $f_p(n)$ ($p = 1-3$), which rules out the pure reptation mechanism even in the high-M B263 matrix.[18]

We now move on and compare the dielectric and viscoelastic behavior of the dipole-inverted PI chains,

* To whom correspondence should be addressed.

10.1021/ma9800562 CCC: $15.00
Published on Web 09/25/1998

which leads to important insights on the chain dynamics. The global motion of the PI chains results in dielectric as well as viscoelastic relaxation. In the consistent description of these relaxation processes, the segment is chosen to be sufficiently large so that it includes many monomeric units and behaves as an entropic strand. This segment is a stress-generating unit on long time scales and is referred to as the *subchain* in the remaining part of this paper. The motion of the subchain after imposition of a *small step strain* (i.e., in the linear regime) is identical to the equilibrium motion. For a chain subjected to this strain at $t = 0$, fundamental features of the slow, linear viscoelastic relaxation are described by the orientation function representing the orientational anisotropy of the subchain at $t > 0$:[17,19c]

$$S(n,t) = (1/a^2)\langle u_x(n,t)\, u_y(n,t)\rangle \qquad (t > 0) \qquad (3)$$

Here, the shear and shear gradient directions are taken as the x and y directions, and $u_x(n,t)$ and $u_y(n,t)$ are the x and y components of the bond vector (end-to-end vector) $\mathbf{u}(n,t)$ of the nth subchain. The average stress arising from the anisotropy of the nth subchain is given by $3kTS(n,t)$ (k = Boltzmann constant, T = absolute temperature),[19c] and this stress relaxes when the anisotropy vanishes (due to the equilibrium chain motion in the linear regime). This relationship between the stress and $S(n,t)$ leads to the stress-optical rule.[19c,23]

The fundamental functions describing the dielectric and viscoelastic relaxation, $C(n,t;m)$ and $S(n,t)$, are related to the first- and second-order moments of $\mathbf{u}(n,t)$, the bond vector *at time t* (see eqs 1 and 3). Thus, the motion of the PI chain is reflected differently in these functions. Utilizing this difference, we can examine changes in the bond vectors of two subchains in a short interval of time.[15,17] These changes are perfectly correlated if the subchains move *coherently* in this interval, while the changes are uncorrelated for the case of an *incoherent* subchain motion. For these two extreme cases of subchain motion, we can explicitly calculate the linear viscoelastic moduli $G^*_{\rm coh}$ and $G^*_{\rm incoh}$ from the dielectrically determined $f_p(n)$ and τ_p.[15,17] Comparison of these moduli with the G^* data enables us to experimentally specify the coherence of the subchain motion.

For PI chains in solutions, we utilized this strategy and found that the short-time motion of the subchains is incoherent in the nonentangled solutions and some degree of coherence emerges in entangled solutions.[17] However, even for the case of well-entangled PI in a monodisperse bulk state ($M/M_e \cong 10$ and 28), imperfect coherence was found.[17] This result reminds us that the constraint release (CR) mechanism makes a considerable contribution to the viscoelastic relaxation of chains in monodisperse systems with M/M_e as large as 30.[14,24,25] Upon removal of the constraints, the subchains would acquire the freedom to move in a more or less random (uncorrelated) way. Thus, the CR mechanism could lead to a lack of perfect coherence of the subchain motion even in these well-entangled systems.

To examine this hypothesis about the CR effect on the coherence of the subchain motion, we compare the viscoelastic and dielectric quantities for dilute PI chains ($M = 48800$) in various environments having different extents of the CR contributions to the PI relaxation. In section II, we summarize the theoretical framework and strategy of this study. In section III, we explain experimental procedures. In section IV, we present the viscoelastic data of the dilute PI chains in the high-M and low-M PB matrices (B263 and B9). In section V, we calculate these moduli and compare the results with the G^* data of the PI chain. We also make a direct comparison of the mechanical and dielectric loss data. We conclude with a summary of our study in section VI.

II. Theoretical Section

II-1. General. Relationships between the dielectric and viscoelastic quantities have been derived for the two extreme cases of coherent and incoherent subchain motion.[15,17] For convenience, this section summarizes the results for *entangled* linear chains with molecular weight M and concentration c.

To describe the global motion of an entangled chain, we naturally choose the entanglement segment as the subchain, the stress-generating unit for slow viscoelastic relaxation. For a chain composed of N subchains ($N = M/M_e$; M_e = molecular weight between entanglements), we consider a change in the subchain bond vector $\mathbf{u}$ in a short interval of time between t and $t + \Delta t$. This change is generally determined by the chain conformation at time t and described by a time-evolution equation of the form[17]

$$\mathbf{u}(n,t+\Delta t) = L^*(n;\Delta t)\, \mathbf{u}(n,t) + \text{thermal noise term} \qquad (4)$$

Here, $L^*(n;\Delta t)$ (=1 for $\Delta t = 0$) is an operator acting on $\mathbf{u}$ at time t: L^* is determined by the nature of the global chain dynamics and the operation $L^*\mathbf{u}$ may involve either local or nonlocal operations (or both).[15] Equation 4 enables us to formulate time evolution equations (in the continuous limit) for the local correlation function and orientation function. Solving these equations, we can find expressions for dielectric and viscoelastic quantities.

II-2. Expression for ϵ''. For the local correlation function $C(n,t;m)$, the time evolution equation derived from eq 4 is[17]

$$\frac{\partial}{\partial t} C(n,t;m) = L_C(n)\, C(n,t;m) \qquad (5)$$

Here, the operator L_C is defined in terms of L^* (eq 4) as

$$L_C(n) = \left[\frac{\partial\langle L^*(n;\Delta t)\rangle}{\partial \Delta t}\right]_{\Delta t \to 0} \qquad (6)$$

Under a boundary condition representing random orientation at the chain ends ($C(n,t;m) = 0$ for n, $m = 0$ and N), the eigenfunctions $f_p(n)$ and the relaxation times τ_p accompanying eq 5 are determined by[17]

$$L_C(n)\, f_p(n) = -[1/\tau_p] f_p(n) \qquad (f_p(0) = f_p(N) = 0) \qquad (7)$$

From the symmetry of the orientational correlation, $\langle \mathbf{u}(n,t)\cdot\mathbf{u}(m,0)\rangle = \langle \mathbf{u}(m,t)\cdot\mathbf{u}(n,0)\rangle$, the solution of eq 5 is written in a form of eigenmode expansion given by eq 2.[6] (The $f_p(n)$ used in eq 2 are normalized so as to satisfy an initial condition representing the Gaussian conformation of the chain, $C(n,0;m) = \delta_{nm}$.[6,18])

From this solution, we obtain an expression for the dielectric loss ϵ'' of PI chains at an angular frequency ω in terms of $f_p(n)$ and τ_p.[6,10,15,17] Specifically, for *regular* PI chains having no dipole inversion, we find[17]

$$\epsilon''(\omega) = 2\Delta\epsilon\sum_{p=1}^{N}\left[\frac{1}{N}\int_0^N f_p(n)\,dn\right]^2 \frac{\omega\tau_p}{1+\omega^2\tau_p{}^2} \quad (8)$$

Here, $\Delta\epsilon$ is the total dielectric intensity for the global chain motion.

II-3. Expression for *G.** For a chain subjected to a small step shear strain at $t = 0$, we consider orientational relaxation at $t > 0$. We define an orientation function for two different subchains:

$$S_2(n,m,t) = (1/a^2)\langle u_x(n,t)u_y(m,t)\rangle \quad (=S(n,t) \quad \text{for} \quad n = m) \quad (9)$$

For this function, the time evolution equation deduced from eq 4 is written as[17]

$$\frac{\partial}{\partial t}S_2(n,t;m) = L_S(n;m)\,S_2(n,t;m) \quad (10)$$

Here, L_S is an operator defined in terms of L^* (eq 4):

$$L_S(n;m) = \left[\frac{\partial\langle L^*(n;\Delta t)L^*(m;\Delta t)\rangle}{\partial\Delta t}\right]_{\Delta t\to 0} \quad (11)$$

This L_S is given as the second-order moment of L^* while the operator L_C for C (eq 6) includes the first-order moment. Thus, a relationship between L_S and L_C changes with the stochastic nature of the chain dynamics represented by L^*, implying that the solution of eq 10 cannot be generally expressed in terms of $f_p(n)$ and τ_p defined for $C(n,t;m)$. However, for two extreme cases, we obtain specific expressions.

For the case of *incoherent* subchain motion where the short time motions of two subchains in individual chains are not correlated at all, eq 11 is decoupled as $L_S(n;m) = L_C(n) + L_C(m)$. For this case, we can explicitly expand $S_2(n,m,t)$ with respect to f_p and τ_p and obtain the relaxation modulus $G(t)$ ($\propto\int_0^N S_2(n,n,t)\,dn$).[17] The resulting expression for the reduced linear viscoelastic modulus, $G_r^* = G^*M/cRT$ (R = gas constant), is[17]

$$G^*_{r,incoh}(\omega) = 2\sum_{p=1}^{N}\left[\frac{1}{N}\int_0^N\{f_p(n)\}^2\,dn\right]\frac{i\omega\tau_p/2}{1+i\omega\tau_p/2} \quad (i=\sqrt{-1}) \quad (12)$$

For the other case of *coherent* subchain motion where the subchain motions are perfectly correlated in individual chains to satisfy a relationship, $[\langle L^*(n;\Delta t)L^*(m;\Delta t)\rangle S_2(n,m,t)\,]_{n=m} = \langle L^*(n;\Delta t)\rangle S_2(n,n,t) + O(\Delta t^2)$, $S_2(n,m,t)$ is expanded differently with respect to f_p and τ_p. For this case, G_r^* is given by[17]

$$G^*_{r,coh}(\omega) = \left(\frac{2G_0M}{cRT}\right)\sum_{p=1}^{N}\left[\frac{1}{N}\int_0^N f_p(n)\,dn\right]^2\frac{i\omega\tau_p}{1+i\omega\tau_p} \quad (13)$$

Here, G_0 is the plateau modulus of the chains having molecular weight M and concentration c (in mass/volume units). In eqs 12 and 13, we have used an expression of G_0 for affine deformation, $G_0 = cRT/M_e = NcRT/M$. (If we use the Doi−Edwards expression, $G_0 = 4cRT/5M_e$, eq 12 is slightly modified (the front factor of 2 becomes $^8/_5$)[15] but eq 13 remains the same.[17])

The calculated moduli are quite different for the above two cases, and we can examine the coherence of the subchain motion by comparing these moduli with the G_r^* data. The coherence can also be examined through a direct comparison of the ϵ'' and G'' data: *If the subchain motion is coherent*, these data of regular PI chains (with no dipole inversion) obey a simple relationship[17] (cf. eqs 8 and 13)

$$\epsilon''(\omega)/\Delta\epsilon = G''(\omega)/G_0 \quad \text{(for regular PI)} \quad (14)$$

Thus, we can conclude that some degree of incoherence exists if a difference is found between the $\epsilon''(\omega)/\Delta\epsilon$ and $G''(\omega)/G_0$ data.

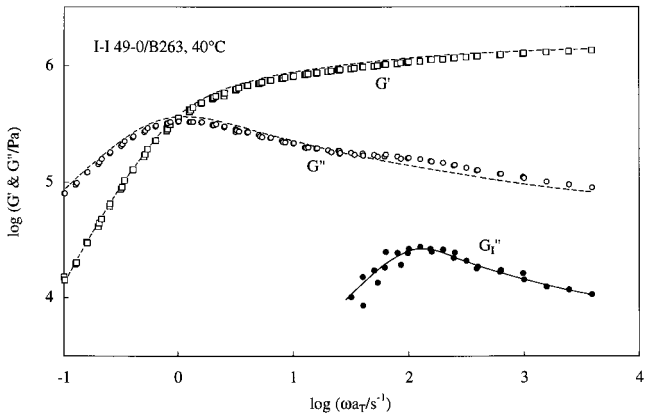

Figure 1. Linear viscoelastic moduli of the I-I 49-0/B263 blend ($\phi_{PI} = 0.05$) at 40 °C (unfilled symbols). The dashed curves indicate the moduli of the bulk B263 matrix. The filled circles indicate the loss moduli G_I'' of the dilute I-I 49-0 chains in the blend evaluated from eq 15.

III. Experimental Section

A regular PI sample, I-I 49-0 (M = 48800), and two polybutadiene samples, B263 (M = 263000) and B9 (M = 9240) were used. The molecular characteristics of these samples were summarized in Table 1 of Part 1.[18]

Linear viscoelastic measurements were carried out with laboratory rheometers (ARES and RMS 605, Rheometrics) in a parallel-plate geometry of diameter =2.5 cm. Storage and loss moduli, G' and G'', were determined for homogeneous blends of I-I 49-0 (with the volume fraction $\phi_{PI} = 0.05$) in the B263 and/or B9 matrices prepared with the method explained in Part 1[18] and also for bulk B263 and B9 matrices. The moduli were measured also for the bulk I-I 49-0 system, and the results were in excellent agreement with the previous data.[17] Time−temperature superposition worked very well for all these G' and G'' data, and the data were reduced to T_r = 40 °C and directly compared with the dielectric data of the same systems obtained in Part 1[18] and in previous studies.[6,15]

The shift factors $a_{T,G}$ for G^* was the same for the I-I 49-0/B263 and I-I 49-0/B9 blends as well as for respective matrices in the bulk state. The $a_{T,G}$ data for the I-I 49-0/B263 blend and bulk B263 matrix, shown in Figure 2 of Part 1,[18] coincided with $a_{T,\epsilon}$ for ϵ'' of the I-I 49-0 chains in the B263 matrix. This result strongly suggests that the dilute I-I 49-0 chains (ϕ_{PI} = 0.05) were uniformly mixed with the B263 matrix. Similar results were found for the I-I 49-0/B9 blend[15] and other PI/PB blends containing dilute PI chains.[13]

IV. Results

IV-1. Overview for Viscoelastic Behavior of I-I 49-0/PB Blends. Figures 1 and 2, respectively, show the master curves of linear viscoelastic moduli for the I-I 49-0/B263 and I-I 49-0/B9 blends at 40 °C. The unfilled squares and circles indicate G_b' and G_b'' of the blends. For comparison, the moduli G_m' and G_m'' of respective matrices *in the bulk state* are shown with the

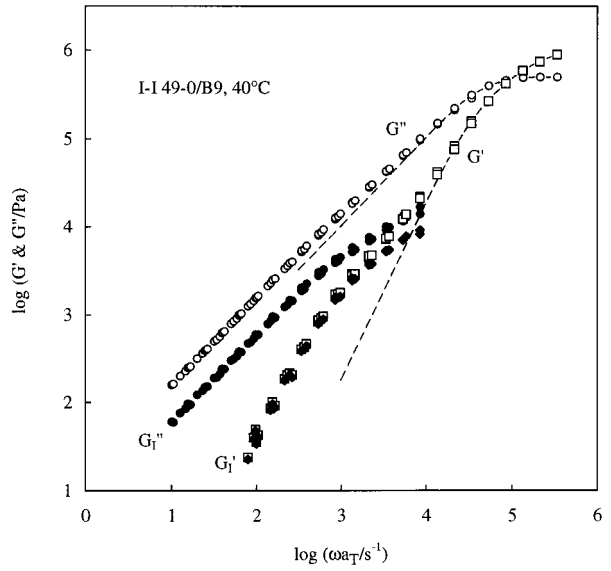

Figure 2. Linear viscoelastic moduli of the I-I 49-0/B9 blend ($\phi_{PI} = 0.05$) at 40 °C (unfilled symbols). The dashed curves indicate the moduli of the bulk B9 matrix. The filled symbols indicate the moduli G_I^* of the dilute I-I 49-0 chains in the blend evaluated from eq 15.

dashed curves. The dilute I-I 49-0 chains ($\phi_{PI} = 0.05$) are entangled only with the B263 and/or B9 matrices; we establish this in a subsequent section (eq 19). The constraint release mechanism makes a negligible contribution to the relaxation of the dilute I-I 49-0 chains in the B263 matrix while it dominates the relaxation in the B9 matrix.[18]

In Figure 1, we note that G_b'' is larger than G_m'' and exhibits a shoulder at $\omega a_T > 20$ s^{-1} where G_m' shows a well-defined rubbery plateau. At lower ωa_T, G_b'' becomes smaller than G_m''. These results indicate that the blend has a fast relaxation process of small intensity that is absent in the bulk matrix. This relaxation process is also seen for the G' data, though less prominently. (In general, G'' has a higher sensitivity to fast and weak relaxation modes than G'.)

The fast and weak relaxation process seen above corresponds to the relaxation of the dilute I-I 49-0 chains in the blend: At ωa_T well above 20 s^{-1}, the I-I 49-0 chains hardly relax and effectively contribute to G_b' of the blend. On the other hand, at $\omega a_T < 20$ s^{-1}, these chains completely relax and work as a "solvent" for the much longer B263 chains. The difference between G_b^* and G_m^* at low ωa_T reflects this "solvent-like" role of I-I 49-0 for the terminal relaxation of the B263 matrix.

In Figure 2, we note a different feature for the I-I 49-0/B9 blend. For this case, the I-I 49-0 relaxation is slower than the matrix relaxation. Thus, the difference between the blend (unfilled symbols) and bulk matrix (dashed curve) is more prominently observed for G' than for G'' (because slow and weak relaxation modes are more sensitively detected in G'). At $\omega a_T < 10^4$ s^{-1}, G_b' is significantly larger than G_m' and exhibits a clear shoulder while G_b'' is only modestly larger than G_m''. This shoulder corresponds to the terminal relaxation of I-I 49-0 in the B9 matrix. These results indicate that the B9 matrix chains, which are *much shorter* than the I-I 49-0 chain, work as the "solvent" for the terminal relaxation of I-I 49-0. This type of matrix behavior has been noted in other blend systems.[14,24−28]

IV-2. Evaluation of G_I^* for I-I 49-0 in PB Matrices. From the G_b^* and G_m^* data shown in Figures 1 and 2, the viscoelastic moduli G_I^* of the dilute I-I 49-0 chains in the B263 and B9 matrices are evaluated in the following way.

IV-2.1. G_I^* in the B9 Matrix. The coincidence of G_m^* and G_b^* at $\omega a_T > 10^4$ s^{-1} (Figure 2) indicates that the dilute I-I 49-0 chains do not affect the terminal relaxation of the B9 chains. Thus, the contribution of the B9 matrix to the viscoelastic modulus of the blend is given by $\phi_m G_m^*(\omega)$, where ϕ_m (=0.95) is the matrix volume fraction in the blend and $G_m^*(\omega)$ is the modulus of bulk B9. At $\omega a_T < 10^4$ s^{-1} where the I-I 49-0 chains exhibit their terminal relaxation, the B9 chains have fully relaxed and work as a "solvent" for the I-I 49-0 chains. In this range of ωa_T, G_I^* is simply evaluated by subtracting the matrix contribution from the G_b^* data:

$$G_I^*(\omega) = G_b^*(\omega) - \phi_m G_m^*(\omega) \tag{15}$$

The validity of this subtraction has been confirmed in previous studies on long, dilute probe chains entangled with much shorter matrix chains.[14,24−28]

At $\omega a_T < 10^4$ s^{-1}, G_I' and G_I'' thus evaluated are shown in Figure 2 with filled diamonds and filled circles, respectively. Since G_b' (unfilled squares) is significantly larger than G_m' (dashed curve) and G_I' is close to G_b' in this range of ωa_T, uncertainties in the evaluation of G_I' are negligibly small. Although G_b'' (unfilled circles) is not much larger than G_m'' (dashed curve), G_I' and G_I'' obtained from eq 15 exhibit the Kramers−Kronig-type consistency[29] in their ω dependence (that resembles the dependence deduced from bead-spring models). This result strongly suggests that G_I'' is also evaluated satisfactorily. In particular, at sufficiently low ωa_T (<100 s^{-1}) where the blend and bulk matrix exhibit respective zero shear viscosities, $\eta_{0,b}$ and $\eta_{0,m}$, G_I'' is accurately evaluated from eq 15 as $G_I''(\omega) = \omega[\eta_{0,b} - \phi_m\eta_{0,m}]$.

IV-2.2. G_I^* in the B263 Matrix. In the B263 matrix, the I-I 49-0 chains relax at $\omega a_T > 20$ s^{-1}; see Figure 1. The evaluation of G_I^* in this matrix requires some molecular considerations. Specifically, we consider the evaluation in two cases.

Case 1: If the dilute I-I 49-0 chains do not affect the relaxation behavior of the B263 matrix at $\omega a_T > 20$ s^{-1}, $G_I^*(\omega)$ is given by eq 15 with G_m^* being the modulus of the bulk B263 matrix. The $G_I''(\omega)$ data evaluated in this way are shown in Figure 1 with filled circles. Since G_b' and G_m' are close to each other, the G_I' evaluated from eq 15 exhibited a large scatter. Those G_I' data are not shown in Figure 1.

Case 2: If the dilute I-I 49-0 chains work exactly as a "solvent" for the B263 matrix at $\omega a_T > 20$ s^{-1}, $G_I^*(\omega)$ is obtained by subtracting the modulus $G_{sol}^*(\omega)$ of a "solution" of B263 (with the volume fraction $\phi_m = 0.95$) from the $G_b^*(\omega)$ data. Since ϕ_m is close to unity and the "solvent" is the polymeric I-I 49-0 that is chemically similar to B263, we may consider the segmental friction of B263 in this solution to be identical to that in bulk B263. For this case, $G_{sol}^*(\omega)$ of the B263 solution is given by[14,26,28]

$$G_{sol}^*(\omega) = \phi_m{}^2 G_m^*(\phi_m{}^{1.5}\omega) \tag{16}$$

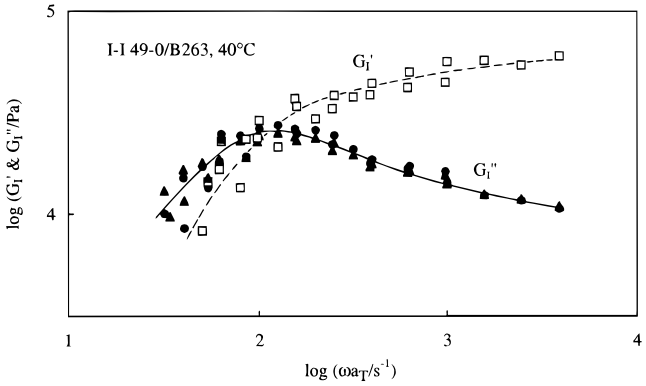

Figure 3. Comparison of the linear viscoelastic moduli G_I^* of the I-I 49-0 chains ($\phi_{PI} = 0.05$) in the B263 matrix evaluated from eq 15 (filled circles) and eq 17 (filled triangles and unfilled squares). The G_I^* evaluated from eq 17 are multiplied by a factor of 0.75. The solid and dashed curves are shown as a guide for eye.

where $G_m^*(\omega)$ is the modulus of bulk B263 at the frequency ω. In eq 16, the front factor, ϕ_m^2, accounts for the dilution of B263 to the volume fraction ϕ_m and the increase of M_e ($\propto \phi_m^{-1}$) on this "dilution", and the factor $\phi_m^{1.5}$ multiplying ω accounts for acceleration of the B263 relaxation due to this increase of M_e. In fact, $G_{sol}^*(\omega)$ given by eq 16 agrees very well with the G_b^* data at low $\omega a_T < 5\ s^{-1}$ where the I-I 49-0 chains fully relax and actually work as the solvent for the B263 chains (cf. Figure 1). We thus evaluate $G_I^*(\omega)$ as

$$G_I^*(\omega) = G_b^*(\omega) - \phi_m{}^2 G_m^*(\phi_m{}^{1.5}\omega) \qquad (17)$$

Validity of Equation 15: At sufficiently high ω where the dilute I-I 49-0 chains have not relaxed, the behavior of the B263 matrix chains in the blend should be close to the behavior in their bulk system. These B263 chains begin to adjust their M_e in the blend to that in the solution after the I-I 49-0 relaxation is completed, and this adjustment requires some time. Thus, during the I-I 49-0 relaxation at $\omega a_T > 20\ s^{-1}$, the behavior of the B263 chains in the blend would be essentially the same as that in their bulk system. This argument suggests that case 1 is close to the real situation and the G_I^* evaluated from eq 15 is to be used as the modulus for the I-I 49-0 chains in the B263 matrix.

Here, we examine an uncertainty of the G_I^* evaluated for case 1 (eq 15) by comparing this G_I^* with the G_I^* for case 2 (eq 17): Among all possibilities for the evaluation of G_I^*, eq 15 gives the lower bound on G_I^* while eq 17 gives the upper bound. Thus, the true modulus of I-I 49-0 is determined from eq 15 with no uncertainty if the two G_I^* obtained from eqs 15 and 17 are indistinguishable. This comparison is made in Figure 3. The G_I'' for the case 1 (eq 15) is shown with the filled circles. The G_I'' for case 2 (eq 17) exhibited a peak that was ≅25% higher than the peak of G_I'' for case 1. For the best comparison of the viscoelastic mode distribution (ω dependence of G_I^*) for cases 1 and 2, G_I' and G_I'' for case 2 are *multiplied by a factor of 0.75* and shown with unfilled squares and filled triangles. Good agreement is found for the filled circles and triangles over the entire range of ω examined. This result demonstrates that the true viscoelastic mode distribution of the I-I 49-0 chain is satisfactorily determined by eq 15. In addition, the agreement suggests that the G_I'' determined by eq 15 includes the uncertainty of less than 25%. Thus, we can safely use this G_I'' in tests of the coherence of the subchain motion.

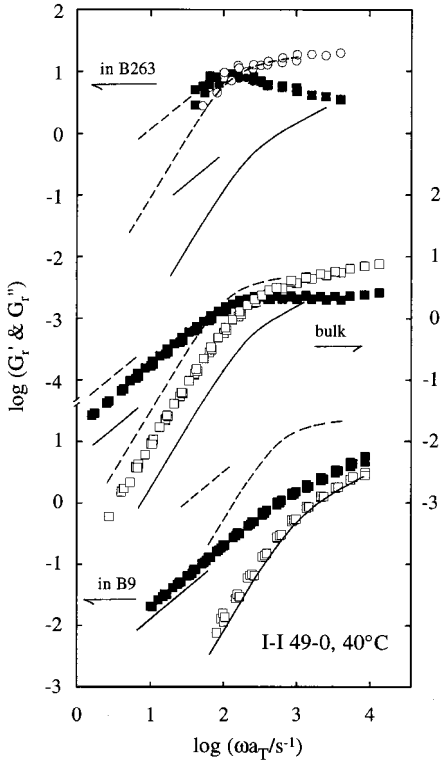

Figure 4. Comparison of $G_{r,incoh}^*$ (solid curves; eq 12) and $G_{r,coh}^*$ (dashed curves; eq 13) evaluated from the dielectrically determined $f_p(n)$ and τ_p ($p = 1-3$)[6,15,18] with the G_r^* data of the I-I 49-0 chain. The comparison is made in the three environments at 40 °C. For evaluation of the G_r^* data, see the text.

The argument for the B263 matrix relaxation at $\omega a_T > 20\ s^{-1}$ suggests that the G_I' for the case 1 (eq 15) is the true storage modulus of the I-I 49-0 chains in this matrix. However, direct application of eq 15 to the G_b^* and G_m^* data resulted in scattered estimates of G_I'. The results shown in Figure 3 enable us to avoid this difficulty. The G_I' and G_I'' for case 2 (eq 17) exhibit the Kramers−Kronig-type consistency[29] in their ω dependence (cf. unfilled squares and filled triangles), and the latter multiplied by the factor of 0.75 coincides well with the true G_I'' determined by eq 15. These results indicate that the true G_I' (for case 1) can be evaluated as the G_I' for case 2 multiplied by the same factor. Thus, G_I' and G_I'' for case 2 multiplied by 0.75 are used later in Figure 4 as the true moduli of the I-I 49-0 chains.

V. Discussion

V-1. Entanglement Spacing for I-I 49-0 in PB Matrices. In Figure 1, the G_I'' data for the dilute I-I 49-0 chains in the B263 matrix (determined by eq 15) exhibit a sharp peak; see filled circles. Thus, we can evaluate the plateau modulus $G_{0,I}$ of these chains as $G_{0,I} = (2/\pi)\int_{-\infty}^{\infty} G_I''\,d(\ln \omega)$. From this $G_{0,I}$, the entanglement spacing (or the molecular weight between entanglements) for the I-I 49-0 chains is obtained as $M_{e,I} = \rho_b \phi_{PI} RT/G_{0,I}$ (ρ_b = density of the blend). For the solid curve smoothly connecting the G_I'' data points in Figure 1, the above integration was numerically carried out to give

$$G_{0,I} \cong 7.0 \times 10^4 \text{ Pa for dilute I-I 49-0 in PB } (\phi_{PI} = 0.05) \quad (18)$$

$$M_{e,I} \cong 1700 \text{ for dilute I-I 49-0 in PB} \quad (19)$$

Since G_0 and M_e of monodisperse systems are independent of the molecular weight,[29,30] G_0 and M_e are determined by local topological interactions of the chains. Thus, G_0 and M_e of I-I 49-0 in both B263 and B9 matrices should be given by eqs 18 and 19.

Note that the $M_{e,I}$ value is close to the $M^\circ_{e,B}$ value (=1900)[30] for bulk PB. For *dilute* PI chains in entangling PB matrices, a previous study[16] determined a hypothetical monodisperse state as a state where the PI chains and PB matrices have the same relaxation time. This state was found to be realized when the PI and PB chains have the same molecular weight, meaning that the dynamics of the dilute PI chains is equivalent to the dynamics of the PB matrix chains having the same M. This result appears to be in harmony with the above coincidence of $M_{e,I}$ and $M^\circ_{e,B}$.

From the $M_{e,I}$ value given by eq 19, we can specify a critical PI molecular weight $M_{c,I}$ that is required for PI chains in the PB matrix to be entangled among themselves. In usual solutions, the chains with a volume faction ϕ are entangled among themselves if their M is larger than $M^\circ_c/\phi \cong 2M^\circ_e/\phi$,[29,30] where M°_c and M°_e are the characteristic molecular weight and entanglement spacing in the bulk state. Applying this criterion to the PI chains in PB matrices and using the above $M_{e,I}$ value, we find that the PI chains of $\phi_{PI} = 0.05$ are entangled among themselves if their M_I is larger than $2M_{e,I}/\phi_{PI} \cong 68000$. According to this result, the PI chains are not entangled among themselves *in any* of the PI/PB blends used in Part 1[18] and Part 2 (this paper).

V-2. Calculation of $G^*_{r,coh}$ and $G^*_{r,incoh}$. For the I-I 49-0 chains in the B9 matrix ($\phi_{PI} = 0.05$) as well as in their monodisperse bulk system, the eigenfunctions $f_p(n)$ and the relaxation times τ_p ($p = 1-3$) of the local correlation function (eq 2) have been determined in previous studies.[6,15,17] In these studies, the integrated eigenfunctions $F_p(n^*)$ were obtained from analyses of ϵ'' data of dipole-inverted PI chains, and $f_p(n)$ were evaluated from numerical differentiation of $F_p(n^*)$

$$F_p(n^*) = \frac{\sqrt{2}}{N}\int_0^{n^*} f_p(n)\,dn, \quad f_p(n) = \frac{1}{\sqrt{2}}\left(\frac{dF_p(n)}{d(n/N)}\right) \quad (20)$$

For the I-I 49-0 chains in the B263 matrix ($\phi_{PI} = 0.05$), $\Delta F_p(n^*) = F_p(n^*) - F_p(N/2)$ and τ_p for the lowest three eigenmodes ($p = 1-3$) were obtained in Part 1.[18] As before,[15,17] we carried out the numerical differentiation (eq 20) for the solid curves shown in Figure 6 of Part 1 that smoothly connect the $\Delta F_p(n^*)$ data points.

For the I-I 49-0 chains in the above three environments, we utilized the $f_p(n)$ and τ_p data for $p = 1-3$ to calculate the reduced moduli for the two extreme cases of incoherent and coherent subchain motion, $G^*_{r,incoh}$ (eq 12) and $G^*_{r,coh}$ (eq 13). The $G^*_{r,incoh}$ and $G^*_{r,coh}$ thus obtained are different from (smaller than) the moduli contributed from all eigenmodes ($p = 1-N$). For $G'_{r,incoh}(\omega)$ rather insensitive to fast eigenmodes, this difference is negligibly small at $\omega < 6/\tau_{1,G}$ where $\tau_{1,G}$ is the longest relaxation time of $G^*_{r,incoh}$.[17,31] Since the intensity factor for $G'_{r,coh}$ ($\propto[(1/N)\int_0^N f_p(n)\,dn]^2$; eq 13) decays with increasing p more strongly than the factor for $G'_{r,incoh}$ ($\propto(1/N)\int_0^N\{f_p(n)\}^2\,dn$; eq 12), the difference between the moduli calculated for $p = 1-3$ and $p = 1-N$ is smaller for $G'_{r,coh}$ than that for $G'_{r,incoh}$. Thus, at $\omega < 6/\tau_{1,G}$, we can safely compare these storage moduli calculated for $p = 1-3$ with the G'_r data.

The situation is somewhat different for the loss modulus which is more significantly contributed from fast eigenmodes than the storage modulus. In the zero shear regime at $\omega < 1/\tau_{1,G}$, the difference between the loss moduli calculated for $p = 1-3$ and $p = 1-N$ is estimated to be $\cong$20%[31] for $G''_{r,incoh}$ and $\cong$10%[32] for $G''_{r,coh}$. This difference specifies an error in the G''_r calculated for $p = 1-3$. For both $G''_{r,incoh}$ and $G''_{r,coh}$, the error becomes larger at higher ω. Thus, we compare the $G''_{r,incoh}$ and $G''_{r,coh}$ calculated for $p = 1-3$ with the G''_r data only in the zero shear regime, keeping in mind the small errors of these $G''_{r,incoh}$ and $G''_{r,coh}$.

V-3. CR Effects on Coherence of Subchain Motion. In Figure 4, we compare the calculated moduli, $G^*_{r,incoh}$ (solid curves) and $G^*_{r,coh}$ (dashed curves), with the G^*_r data at 40 °C for the I-I 49-0 chains in the B263 and B9 matrices and in the monodisperse bulk system. The $G'_{r,incoh}$ and $G'_{r,coh}$ are shown at $\omega < 6/\tau_{1,G}$ while the $G''_{r,incoh}$ and $G''_{r,coh}$ (the short straight lines with slope of unity) are shown only in the zero shear regime for the reasons explained above. The unfilled and filled squares indicate the G'_r and G''_r data: For the bulk I-I 49-0 system, the G^* data obtained in this and previous[17] studies were used to evaluate the reduced modulus $G^*_r = G^*M_I/\rho^\circ_I RT$ (ρ°_I = bulk PI density). For the I-I 49-0 chain in the B263 and B9 matrices, the G^*_I data determined from eq 15 (cf. Figures 1 and 2) were used to evaluate $G^*_r = G^*_I M_I/\rho_b\phi_{PI}RT$ (ρ_b = blend density).

For the I-I 49-0 chain in the B263 matrix, the earlier arguments suggest that the true G''_I is determined by eq 15. However, the ω dependence of this G''_I is almost identical to that of the G''_I determined by eq 17 and the magnitude is larger, by a factor of 25%, for the latter; see Figure 3. Thus, G'_r and G''_r are also evaluated from the G'_I and G''_I determined by eq 17 and multiplied by 0.75: These G'_r and G''_r are shown in Figure 4 with the unfilled circles and filled circles, the latter almost coinciding with the filled squares.

Figure 4 demonstrates the following features of the I-I 49-0 chain in the three environments. In the B9 matrix, $G'_{r,incoh}$ is in excellent agreement with the G'_r data. The agreement of $G''_{r,incoh}$ and the G''_r data is also satisfactory if we consider the small error in the calculated $G''_{r,incoh}$ ($\cong$20%). In contrast, we find significant differences between $G^*_{r,coh}$ and the G^*_r data. Thus, we conclude that the short-time motion of the subchains is incoherent for the dilute I-I 49-0 chains entangled with the highly mobile, low-M B9 matrix.

For the monodisperse bulk I-I 49-0 system, some degree of coherence of the subchain motion is noted from the deviation of $G^*_{r,incoh}$ from the G^*_r data. However, $G^*_{r,coh}$ is also different from the G^*_r data, indicating that the coherence is not perfect in this system.

For the I-I 49-0 chain in the B263 matrix, the G^*_r data may include the small uncertainty explained earlier (less than 25%). The calculated $G^*_{r,coh}$ agrees with the G^*_r data within this uncertainty, while $G^*_{r,incoh}$ exhibits a significant deviation. Thus, the subchain motion is highly coherent for the I-I 49-0 chain in the B263 matrix.

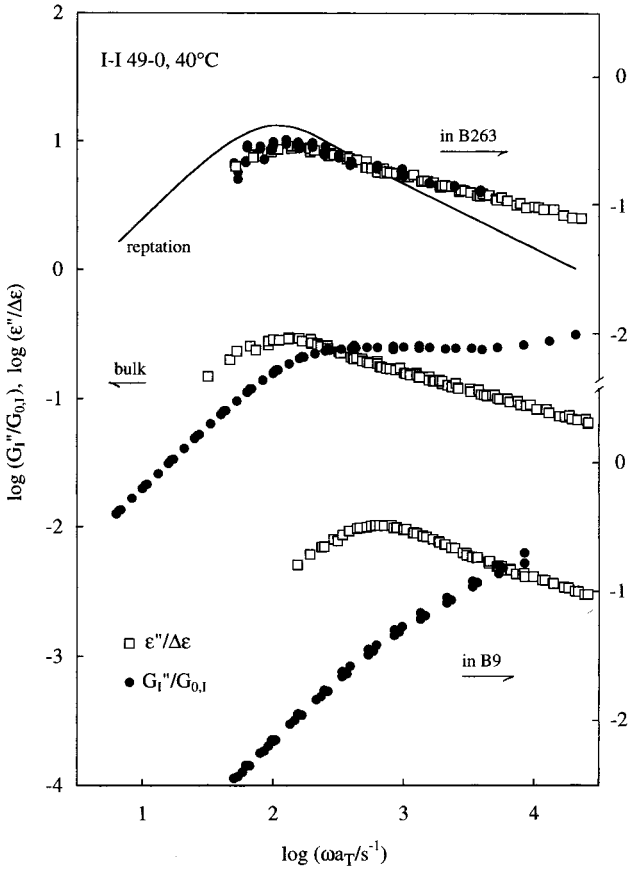

Figure 5. Comparison of the $G_I''/G_{0,I}$ and $\epsilon''/\Delta\epsilon$ data at 40 °C for the I-I 49-0 chain in the three environments as indicated. The solid curve shown for the I-I 49-0 chain in the B263 matrix indicates $G_I''/G_{0,I}$ and $\epsilon''/\Delta\epsilon$ deduced from the pure reptation model. (The frequency scale of this curve is adjusted so that the curve has the maximum at the same frequency as the $G_I''/G_{0,I}$ and $\epsilon''/\Delta\epsilon$ data.)

In Figure 5, we compare the G_I'' and ϵ'' data of the I-I 49-0 chain. According to eq 14, G_I'' is reduced by the plateau modulus, $G_0 = 4.8 \times 10^5$ Pa for bulk I-I 49-0 and $G_{0,I} = 7.0 \times 10^4$ Pa (eq 18) for the I-I 49-0 chains in the B263 and B9 matrices ($\phi_{PI} = 0.05$), while ϵ'' is reduced by the dielectric intensity $\Delta\epsilon$ in respective environments. Since $G_{0,I}$ was evaluated from the G_I'' data, the small uncertainty (<25%) of G_I'' in the B263 matrix (cf. Figure 3) does not affect the results of comparison of the *normalized* losses, $G_I''/G_{0,I}$ and $\epsilon''/\Delta\epsilon$. Thus, in Figure 5, we can clearly examine whether the subchain motion is perfectly coherent or not by comparing these losses over a wide range of ω.

For the I-I 49-0 chain in the B263 matrix, the $G_I''/G_{0,I}$ and $\epsilon''/\Delta\epsilon$ data agree with each other within experimental scatter of the data. Thus, eq 14 is valid. This result confirms that the subchain motion is highly coherent for the dilute I-I 49-0 chains in the B263 matrix. The coherence is incomplete in the bulk I-I 49-0 system and in the B9 matrix, as noted from the differences between the $G_I''/G_{0,I}$ and $\epsilon''/\Delta\epsilon$ data. In fact, Figure 4 demonstrates that the subchain motion is highly incoherent in the B9 matrix. (Note that the comparison in Figure 5 specifies whether the coherence is complete or not. In contrast, the comparison of $G^*_{r,incoh}$ and $G^*_{r,coh}$ with the G^*_r data (Figure 4) specifies whether the subchain motion is perfectly coherent or incoherent.)

The constraint release (CR) contribution to the PI dynamics, measured by the ratio of the CR relaxation time τ_{CR} to the observed longest relaxation time τ_1, is quite different in the three environments: As explained in Part 1,[18] the CR mechanism dominates the PI dynamics in the B9 matrix ($\tau_{CR}/\tau_1 = 1.1$) while it has negligible effects in the B263 matrix ($\tau_{CR}/\tau_1 = 5600$) and modest effects in the monodisperse bulk I-I 49-0 system ($\tau_{CR}/\tau_1 \cong 3.5$). Considering this result and those found in Figures 4 and 5, we can now conclude that the CR contribution to the probe chain dynamics is one of the important factors that determine the short-time coherence of the subchain motion in the probe: The larger this contribution, the smaller the degree of coherence.

We have to emphasize that the magnitude of entanglements measured by the M_I/M_e ratio is not a factor determining the degree of the coherence:[33] This ratio is ≅29 for the dilute I-I 49-0 chains in both B263 and B9 matrices ($M_{e,I} \cong 1700$ for $\phi_{PI} = 0.05$; eq 19) and ≅10 in the bulk I-I 49-0 system ($M^\circ_{e,I} \cong 5000$ for bulk PI[29,30]). Despite the coincidence of the $M_I/M_{e,I}$ ratio in the B263 and B9 matrices, the subchain motion is much more coherent in the former.

V-4. Comparison with the Tube Model. We focus on the I-I 49-0 subchain motion in the B263 matrix (Figure 5). The solid curve shown there is the normalized losses, $G_I''/G_{0,I}$ and $\epsilon''/\Delta\epsilon$, for a chain relaxing by the perfectly coherent, pure reptation mechanism. (The frequency scale for this curve is adjusted so that the curve has the maximum at the same frequency as the $G_I''/G_{0,I}$ and $\epsilon''/\Delta\epsilon$ data.) Despite the high coherence of the subchain motion experimentally found in the B263 matrix, the $G_I''/G_{0,I}$ and $\epsilon''/\Delta\epsilon$ data are significantly different from the pure reptation curve. This difference, found for the *normalized* losses, allows us to conclude that the highly coherent motion of the I-I 49-0 chains in the B263 matrix results from a mechanism other than *pure* reptation. This conclusion is in harmony with that of Part 1.[18]

One may argue that the $M/M_{e,I}$ ratio (≅29) of the I-I 49-0 chain in the B263 matrix is not large enough to allow the purely reptative motion of this chain and that the contour length fluctuation mechanism[19b,c,21,34,35] has a significant contribution to the dynamics of the chain. In fact, a power-law exponent for the data of the I-I 49-0 chain in the B263 matrix at high ω, $G_I''/G_{0,I} = \epsilon''/\Delta\epsilon \propto \omega^{-\alpha}$ with $\alpha \cong 1/4$ (see Figure 5), is in close agreement with the exponent theoretically deduced for the combined mechanism of reptation plus contour length fluctuation.[34] In addition, the M_I dependence of τ_1 for the PI chains in matrices of much longer chains (eq 6 in Part 1)[18] is not far from the dependence deduced for this combined mechanism.[34,35]

However, we have to also note an important fact that the contour length fluctuation results from the Rouse motion of the chain trapped in a fixed tube.[34,35] It is not clear whether the experimentally observed high coherence of the subchain motion in the B263 matrix is consistent with this Rouse motion (that leads to the perfect incoherence under the absence of the tube confinement). In addition, the eigenfunctions $f_p(n)$ for the local correlation function (eq 2) have not been calculated for the combined mechanism of reptation plus contour length fluctuation. Thus, it is not clear whether the experimentally obtained nonsinusoidal $f_p(n)$ can be explained by this mechanism. Further theoretical studies are desirable to clarify these problems.

VI. Concluding Remarks

Comparing viscoelastic and dielectric data from dilute PI chains in various environments, we have examined the short-time coherence of the subchain motion in individual chains. The comparison unequivocally indicated that the constraint release (CR) mechanism is one of the important factors that determine this coherence: The larger the CR contribution to the PI dynamics, the smaller the degree of the coherence. We also found that the coherence is not determined by the magnitude of entanglements measured by the M/M_e ratio. No available molecular models seem to explain these experimental findings. Specifically, it is not clear whether the results can be explained within the framework of the generalized tube model considering the CR, contour length fluctuation, and reptation mechanisms. Further theoretical studies are necessary to clarify this problem.

References and Notes

(1) Imanishi, Y.; Adachi, K.; Kotaka, T. *J. Chem. Phys.* **1988**, *89*, 7585.
(2) Adachi, K.; Yoshida, H.; Fukui, F.; Kotaka, T. *Macromolecules* **1990**, *23*, 3138.
(3) Yoshida, H.; Watanabe, H.; Adachi, K.; Kotaka, T. *Macromolecules* **1991**, *24*, 2981.
(4) Adachi, K.; Kotaka, T. *Prog. Polym. Sci.* **1993**, *18*, 585.
(5) Boese, D.; Kremer, F.; Fetters, L. J. *Macromolecules* **1990,** *23*, 829; Boese, D.; Kremer, F.; Fetters, L. J. **1990**, *23*, 1826.
(6) Watanabe, H.; Urakawa, O.; Kotaka, T. *Macromolecules* **1993**, *26*, 5073.
(7) Yoshida, H.; Adachi, K.; Watanabe, H.; Kotaka, T. *Polym. J. (Jpn.)* **1989**, *21*, 863.
(8) Patel, S. S.; Takahashi, K. M. *Macromolecules* **1992**, *25*, 4382.
(9) Urakawa, O.; Adachi, K.; Kotaka, T. *Macromolecules* **1993**, *26*, 2036; Urakawa, O.; Adachi, K.; Kotaka, T. **1993**, *26*, 2042.
(10) Watanabe, H.; Yamada, H.; Urakawa, O. *Macromolecules* **1995**, *28*, 6443.
(11) Urakawa, O.; Watanabe, H. *Macromolecules* **1997**, *30*, 652.
(12) Adachi, K.; Itoh, S.; Nishi, I.; Kotaka, T. *Macromolecules* **1990**, *23*, 2554.
(13) (a) Watanabe, H.; Yamazaki, M.; Yoshida, H.; Adachi, K.; Kotaka, T. *Macromolecules* **1991**, *24*, 5365. (b) Watanabe, H.; Yamazaki, M.; Yoshida, H.; Kotaka, T. *Macromolecules* **1991**, *24*, 5372.
(14) Watanabe, H.; Kotaka, T. *CHEMTRACTS Macromol. Chem.* **1991**, *2*, 139 and references therein.
(15) Watanabe, H.; Urakawa, O.; Kotaka, T. *Macromolecules* **1994**, *27*, 3525.
(16) Watanabe, H.; Urakawa, O.; Yamada, H.; Yao, M.-L. *Macromolecules* **1996**, *29*, 755.
(17) Watanabe, H.; Yao, M.-L.; Osaki, K. *Macromolecules* **1996**, *29*, 97.
(18) Matsumiya, Y.; Watanabe, H.; Osaki, K.; Yao, M.-L. *Macromolecules* **1998**, *31*, 7528.
(19) (a) Doi, M.; Edwards, S. F. *The Theory of Polymer Dynamics*; Clarendon: Oxford, 1986; Chapter 4; (b) Chapter 6; (c) Chapter 7.
(20) Klein, J. *Macromolecules* **1978**, *11*, 852.
(21) Graessley, W. W. *Adv. Polym. Sci.* **1982**, *47*, 67.
(22) Watanabe, H.; Tirrell, M. *Macromolecules* **1989**, *22*, 927.
(23) Janeschitz-Kriegl, H. *Polymer Melt Rheology and Flow Birefringence*; Springer: New York, 1983.
(24) Watanabe, H.; Sakamoto, T.; Kotaka, T. *Macromolecules* **1985**, *18*, 1436.
(25) Watanabe, H.; Yoshida, H.; Kotaka, T. *Macromolecules* **1988**, *21*, 2175; Watanabe, H.; Yoshida, H.; Kotaka, T. *Macromolecules* **1992**, *25*, 2442.
(26) Watanabe, H.; Kotaka, T. *Macromolecules* **1984**, *17*, 2316.
(27) Watanabe, H.; Kotaka, T. *Macromolecules* **1986**, *19*, 2520.
(28) Watanabe, H.; Yamazaki, M.; Yoshida, H.; Kotaka, T. *Macromolecules* **1991**, *24*, 5573.
(29) Ferry, J. D. *Viscoelastic Properties of Polymers*, 3rd ed.; Wiley: New York, 1980.
(30) Graessley, W. W. *Adv. Polym. Sci.* **1974**, *16*, 55.
(31) The estimate of the difference between $G^*_{r,incoh}$ calculated for $p = 1-3$ and $p = 1-N$ was obtained for the Rouse-type CR model.[17] Although this model does not accurately describe the detailed feature (nonsinusoidal f_p[15,18]) of actual CR relaxation, G^*_r of the model is considerably close to the G^*_r data in the CR regime.[15] Thus, we may apply the above estimate to $G^*_{r,incoh}$ of the PI chains exhibiting the non-Rouse-type CR relaxation.
(32) The difference between $G^*_{r,coh}$ calculated for $p = 1-3$ and $p = 1-N$ was estimated for the reptation model. For any type of coherent subchain motion, the viscoelastic intensity factor ($\propto[(1/N)\int_0^N f_p(n)\,dn]^2$; eq 13) rapidly decays with increasing p because $f_p(n)$ oscillates with n more frequently for larger p, so that $G^*_{r,coh}$ at low ω is dominated by a few slow eigenmodes. Thus, the estimate obtained for the reptation model may be applied to $G^*_{r,coh}$ of the PI chains exhibiting the coherent subchain motion.
(33) For a monodisperse bulk PI system with $M_I = 140000$ ($M_I/M^\circ_{e,I} \cong 28$), G'' and ϵ'' were found to have different ω dependence.[2] Namely, G''/G_0 and $\epsilon''/\Delta\epsilon$ do not agree with each other and the subchain motion exhibits some incoherence in this system. Despite this large $M/M^\circ_{e,I}$ value, the system has a fairly small τ_{CR}/τ_1 ratio $\cong$ 17 (evaluated from eq 9 of Part 1[18]). This τ_{CR}/τ_1 ratio is much smaller than the ratio ($\cong$5600)[18] for the I-I 49-0 chains having nearly the same $M_I/M_{e,I}$ value ($\cong$29) in the B263 matrix, naturally resulting in the imperfect coherence of the subchain motion in the bulk PI system with $M_I = 140000$.
(34) Doi, M. *J. Polym. Sci., Polym. Lett. Ed.* **1981**, *19*, 265.
(35) Doi, M. *J. Polym. Sci., Polym. Phys. Ed.* **1983**, *21*, 667.

MA9800562